DOI: 10.1021/ma9003133

Macromolecules
ARTICLE

# Azobenzene-Containing Linear−Dendritic Diblock Copolymers by Click Chemistry: Synthesis, Characterization, Morphological Study, and Photoinduction of Optical Anisotropy

**Jesús del Barrio,[†] Luis Oriol,*[,†] Rafael Alcalá,[‡] and Carlos Sánchez*[,‡]**

[†]*Departamento de Química Orgánica y Química Física, Facultad de Ciencias-Instituto de Ciencia de Materiales de Aragón, Universidad de Zaragoza-CSIC, 50009 Zaragoza, Spain, and* [‡]*Departamento de Física de la Materia Condensada, Facultad de Ciencias-Instituto de Ciencia de Materiales de Aragón, Universidad de Zaragoza-CSIC, 50009 Zaragoza, Spain*

*Received February 11, 2009; Revised Manuscript Received June 17, 2009*

ABSTRACT: We report here the synthesis of a series of new photoaddressable linear−dendritic diblock copolymers composed of poly(ethylene glycol) (PEG) and the first four generations of dendritic aliphatic polyesters based on 2,2-bis(hydroxymethyl)propionic acid (bis-MPA) functionalized at the periphery with mesogenic and photochromic cyanazobenzene units. The dendritic block was synthesized through a double-stage convergent approach starting from the 2-azidoethyl ester of bis-MPA. Subsequent functionalization of the periphery allowed us to obtain liquid crystalline azodendrons bearing an azide group at the focal point. Finally, the block copolymers (BCs) were obtained by Huisgen's 1,3-dipolar cycloaddition (click chemistry) between the azo-dendrons and an alkyne-functionalized PEG. The chemical structure and low polydispersity of the BCs were checked by nuclear magnetic resonance spectroscopy (NMR), Fourier transform infrared spectroscopy (FT-IR), matrix-assisted laser desorption/ionization time-of-flight mass spectrometry (MALDI-TOF MS), and gel permeation chromatography (GPC). Liquid crystalline properties were analyzed by differential scanning calorimetry (DSC) and polarized-light optical microscopy (POM). The azodendrons showed a smectic phase over a broad temperature range. Mesomorphism was also detected for the BCs except for the BC bearing two cyanoazobenzene units. X-ray diffraction (XRD) experiments demonstrated the lamellar nanosegregation of the diblock copolymers. The lamellar nature of the morphology was also confirmed by transmission electron microscopy (TEM) measurements. Birefringence was induced using 488 nm linearly polarized light on thin films of the BC bearing 16 cyanoazobenzene units under different irradiation conditions. Stable values of the in-plane order parameter up to 0.56 were obtained for this material.

## Introduction

Block copolymers (BCs) are of particular interest in the design of novel functional materials based on self-assembling properties. It is well-known that BCs can form microphase-separated nanostructures with cylindrical, lamellar, spherical, or bicontinuous morphologies.[1−3] On the other hand, the incorporation of liquid crystalline blocks into such systems offers the possibility of altering their self-assembly behavior while allowing the introduction of molecules with optical, electronic, electro-optic, or photoresponsive functionalities. In particular, BCs containing azobenzene units represent an attractive area of research.[4−25,26b,26c,27] Azobenzene molecules undergo isomerization between the *trans* and *cis* states when they are irradiated in their absorption bands. Photoinduced anisotropy generated using linearly polarized light has been thoroughly investigated in azobenzene-containing polymers.[4−12] The confinement of these photoresponsive units in nanosized block copolymer domains gives these materials unique properties that make them interesting in different applications such as volume holographic storage[20,21] or in the preparation of photoresponsive nanoscopic objects.[22] The irradiation of these materials can induce reorientation of individual molecules. Even orientation of nanosized domains themselves by optical means has recently been demonstrated in azobenzene-containing BCs.[23]

*Corresponding authors: Fax +34 976762686, e-mail loriol@unizar.es (L.O.), carloss@unizar.es (C.S.).

In all of these cases, the development of well-defined nanostructures involved the synthesis of BCs with controlled macromolecular architecture, molecular weight distribution, and composition. This achievement has been possible due to the development of controlled polymerization techniques. In particular, azobenzene-containing BCs have commonly been obtained by using techniques such as atom transfer radical polymerization (ATRP),[15−17,21,24−26] ring-opening metathesis polymerization (ROMP),[26a] and reversible addition−fragmentation chain transfer polymerization (RAFT).[27] The reported examples concern BCs with a linear−linear architecture. Alternatively, we present here the synthesis of a new series of linear−dendritic BCs bearing a perfectly controlled number of azobenzene units at the periphery of the dendritic block. This unique macromolecular structure offers the opportunity to combine the perfectly branched architecture and high functionality of dendrimers with the phase separation behavior of traditional linear−linear BCs. The most versatile synthetic strategy in the preparation of linear−dendritic BCs involves direct coupling of preformed end-functionalized linear polymers with reactive dendrons that bear a complementary functional group at their focal point.[28] Although this strategy yields the BC in one step, it is limited by the availability of macromolecular systems with appropriate coupling chemistries. In this context, Sharpless' click chemistry[29] (Huisgen's 1, 3-dipolar cycloaddition[30] between azido and alkynyl groups catalyzed by copper salts) has recently proved to be a very powerful synthetic tool in polymer science due to its high selectivity and almost complete conversion obtained under mild

 Published on Web 07/07/2009 

**Chart 1. Chemical Structure of PEG-AZO*n* Linear−Dendritic Block Copolymers**

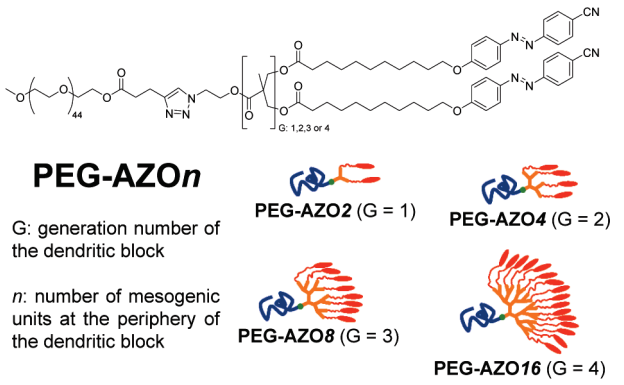


reaction conditions.[31] Numerous studies have demonstrated the applicability of this approach for the synthesis of BCs with linear−linear[32] and linear−dendron-like[33] macromolecular architecture. This versatile synthetic route may pave the way to functional BCs with novel macromolecular architecture.

In this paper, we report on the synthesis of a new class of functional linear−dendritic BCs composed of a linear block of poly(ethylene glycol) (PEG) and the first four generations of aliphatic polyester dendrons functionalized at the periphery with 4-cyanoazobenzene units as the dendritic block (Chart 1). The chemical structures and polydispersity of the BCs were checked by nuclear magnetic resonance (NMR), Fourier transform infrared spectroscopy (FT-IR), matrix-assisted laser desorption/ionization time-of-flight mass spectrometry (MALDI-TOF MS), and gel permeation chromatography (GPC). The mesomorphic properties and morphology of the BCs in bulk have been studied by polarized-light optical microscopy (POM), differential scanning calorimetry (DSC), X-ray diffraction (XRD), and transmission electron microscopy (TEM). A study was also carried out on the photoinduced anisotropy in films of the linear−dendritic BC bearing 16 azobenzene units (Chart 1) using 488 nm linearly polarized light.

## Experimental Section

**Materials.** All starting materials were purchased from Sigma-Aldrich and used without further purification. 11-[4-(4′-Cyanophenylazo)phenyloxy]undecanoic acid and compounds **1** and **5** (see Scheme 1) were synthesized according to previously described methods.[34,35] The synthesis of the first four generations of aliphatic polyester dendrons bearing a single azide group at the focal point and hydroxyl groups at the periphery (compounds **OH*n*** in Scheme 1) was accomplished through a double-stage convergent approach.[35] Details on the synthesis of **OH*n*** and the alkyne-functionalized PEG (compound **8** in Scheme 2) are included in the Supporting Information.

**Synthesis of Azodendrons (AZO*n*).** ***AZO2***. 4-(Dimethylamino)pyridinium *p*-toluenesulfonate (DPTS) (1.23 g, 3.94 mmol), **OH*2*** (0.40 g, 1.97 mmol), and 11-[4-(4′-cyanophenylazo)phenyloxy]undecanoic acid (1.92 g, 4.71 mmol) were dissolved in a mixture of dichloromethane (20 mL) and DMF (10 mL). The reaction flask was flushed with argon, and *N,N*′-dicyclohexylcarbodiimide (DCC) (1.07 g, 5.19 mmol) was added. The mixture was stirred at room temperature (RT) for 24 h under an argon atmosphere. The white precipitate (*N,N*′-dicyclohexylurea) was filtered off, and the solvent was evaporated. The crude product was purified by liquid chromatography on silica gel and eluted with dichloromethane, gradually increasing to 1:40 ethyl acetate:dichloromethane. **AZO*2*** was obtained as an orange powder. Yield: 1.51 g (78%). $^1$H NMR (400 MHz, $CDCl_3$, $\delta$): 7.93 (d, $J$ = 8.9 Hz, 8H), 7.78 (d, $J$ = 8.5 Hz, 4H), 7.01 (d, $J$ = 8.9 Hz, 4H), 4.32−4.19 (m, 6H), 4.05 (t, $J$ = 6.5 Hz, 4H), 3.48 (t, $J$ = 5.0, 2H), 2.31 (t, $J$ = 7.6, 4H), 1.87−1.77 (m, 4H), 1.65−1.54 (m, 4H), 1.52−1.41 (m, 4H), 1.40−1.20 (m, 23H). $^{13}$C NMR (100 MHz, $CDCl_3$, $\delta$): 173.19, 172.56, 162.71, 154.77, 146.65, 133.12, 125.43, 123.03, 118.63, 114.84, 113.09, 68.45, 65.14, 63.71, 49.66, 46.43, 34.06, 29.46, 29.34, 29.31, 29.20, 29.11, 29.07, 25.96, 24.83, 17.68. IR (KBr, cm$^{-1}$): 2220, 2102, 1741, 1601, 1255, 845. MALDI-TOF MS (matrix: dithranol) Calcd for $C_{55}H_{67}N_9O_8$: 982.18. Found: 982.6 $[M]^+$, 1005.6 $[M + Na]^+$. Anal. Calcd for $C_{55}H_{67}N_9O_8$: C, 67.26; H, 6.88; N, 12.83. Found: C, 67.42; H, 7.00; N, 12.42.

***AZO4***. DPTS (1.44 g, 4.60 mmol), **OH*4*** (0.50 g, 1.15 mmol), DCC (1.25 g, 6.06 mmol), and 11-[4-(4′-cyanophenylazo)-phenyloxy]undecanoic acid (2.25 g, 5.52 mmol) were reacted according to the esterification procedure described for **AZO*2*** in a mixture of dichloromethane (25 mL) and DMF (10 mL). The crude product was purified by liquid chromatography on silica gel and eluted with dichloromethane, gradually increasing to 1:20 ethyl acetate:dichloromethane. **AZO*4*** was obtained as an orange powder. Yield: 1.72 g (75%). $^1$H NMR (400 MHz, $CDCl_3$, $\delta$) 7.92 (d, $J$ = 9.1 Hz, 16H), 7.78 (d, $J$ = 8.7 Hz, 8H), 7.00 (d, $J$ = 9.1 Hz, 8H), 4.32−4.26 (m, 6H), 4.22 (d, $J$ = 11.1 Hz, 4H), 4.18 (d, $J$ = 11.1 Hz, 4H), 4.04 (t, $J$ = 6.5 Hz, 8H), 3.51 (t, $J$ = 5.0 Hz, 2H), 2.30 (t, $J$ = 7.6 Hz, 8H), 1.86−1.76 (m, 8H), 1.65−1.53 (m, 8H), 1.51−1.41 (m, 8H), 1.41−1.20 (m, 49H). $^{13}$C NMR (100 MHz, $CDCl_3$, $\delta$): 173.17, 172.03, 171.89, 162.70, 154.76, 146.66, 133.13, 125.43, 123.03, 118.63, 114.83, 113.12, 68.45, 65.63, 64.96, 64.04, 49.61, 46.73, 46.39, 34.00, 29.49, 29.39, 29.34, 29.25, 29.13, 29.10, 25.98, 24.82, 17.78, 17.46. IR (KBr, cm$^{-1}$): 2221, 2105, 1741, 1601, 1254, 836. MALDI-TOF MS (matrix: dithranol) Calcd for $C_{113}H_{137}N_{15}O_{18}$: 1993.39. Found: 1993.7 $[M]^+$, 2016.0 $[M + Na]^+$, 2031.8 $[M + K]^+$. Anal. Calcd for $C_{113}H_{137}N_{15}O_{18}$: C, 68.09; H, 6.93; N, 10.54. Found: C, 68.31; H, 7.00; N, 10.28.

***AZO8***. DPTS (1.60 g, 5.12 mmol), **OH*8*** (0.58 g, 0.64 mmol), DCC (1.40 g, 6.79 mmol), and 11-[4-(4′-cyanophenylazo)phenyloxy]undecanoic acid (2.50 g, 6.13 mmol) were reacted according to the esterification procedure described for **AZO*2*** in a mixture of dichloromethane (30 mL) and DMF (10 mL). The crude product was purified by liquid chromatography on silica gel and eluted with dichloromethane, gradually increasing to 1:10 ethyl acetate:dichloromethane. **AZO*8*** was obtained as an orange powder. Yield: 1.80 g (70%). $^1$H NMR (400 MHz, $CDCl_3$, $\delta$): 7.92 (d, $J$ = 8.9 Hz, 32H), 7.77 (d, $J$ = 8.5 Hz, 16H), 6.99 (d, $J$ = 8.9 Hz, 16H), 4.33−4.11 (m, 30H), 4.02 (t, $J$ = 6.5 Hz, 16H), 3.52 (t, $J$ = 5.0, 2H), 2.29 (t, $J$ = 6.7 Hz, 16H), 1.85−1.74 (m, 16H), 1.65−1.52 (m, 16H), 1.51−1.18 (m, 117H). $^{13}$C NMR (100 MHz, $CDCl_3$, $\delta$): 173.11, 172.01, 171.42, 171.33, 162.67, 154.72, 146.64, 133.12, 125.43, 123.02, 118.61, 114.81, 113.13, 68.42, 65.27, 65.18, 64.82, 64.17, 49.59, 46.68, 46.48, 46.34, 33.98, 29.52, 29.42, 29.37, 29.28, 29.14, 29.13, 26.00, 24.83, 17.79, 17.49, 17.37. IR (KBr, cm$^{-1}$): 2221, 2105, 1741, 1601, 1255, 847. MALDI-TOF MS (matrix: dithranol) Calcd for $C_{229}H_{277}N_{27}O_{38}$: 4015.81. Found: 4015.6 $[M]^+$. Anal. Calcd for $C_{229}H_{277}N_{27}O_{28}$: C, 68.49; H, 6.95; N, 9.42. Found: C, 68.37; H, 6.96; N, 9.18.

***AZO16***. DPTS (1.60 g, 5.12 mmol), **OH*16*** (0.59 g, 0.32 mmol), DCC (1.39 g, 6.74 mmol), and 11-[4-(4′-cyanophenylazo)phenyloxy]undecanoic acid (2.50 g, 6.13 mmol) were reacted according to the esterification procedure described for **AZO*2*** in a mixture of dichloromethane (40 mL) and DMF (10 mL). The crude product was purified by liquid chromatography on silica gel and eluted with dichloromethane, gradually increasing to 1:10 ethyl acetate:dichloromethane. **AZO*16*** was obtained as an orange powder. Yield: 1.57 g (61%). $^1$H NMR (400 MHz, $CDCl_3$, $\delta$): 7.90 (d, $J$ = 8.9 Hz, 64H), 7.76 (d, $J$ = 8.5 Hz, 32H), 6.97 (d, $J$ = 8.9 Hz, 32H), 4.36−4.11 (m, 62H), 4.00 (t, $J$ = 6.5 Hz, 32H), 3.53 (t, $J$ = 4.6 Hz, 2H), 2.28 (t, $J$ = 7.6 Hz, 32H), 1.84−1.74 (m, 32H), 1.64−1.52 (m, 32H), 1.50−1.20 (m, 237H). $^{13}$C NMR (100 MHz, $CDCl_3$, $\delta$): 173.06, 171.98, 171.44, 171.29, 171.22, 162.63, 154.67, 146.63, 133.11, 125.41, 123.01, 118.57, 114.78, 113.16, 65.40, 65.32, 65.02, 64.99, 64.74, 64.31, 49.61, 46.64, 46.41, 46.31, 45.48, 33.98, 29.54,

**Scheme 1. Synthesis of the Azodendrons, AZO*n***

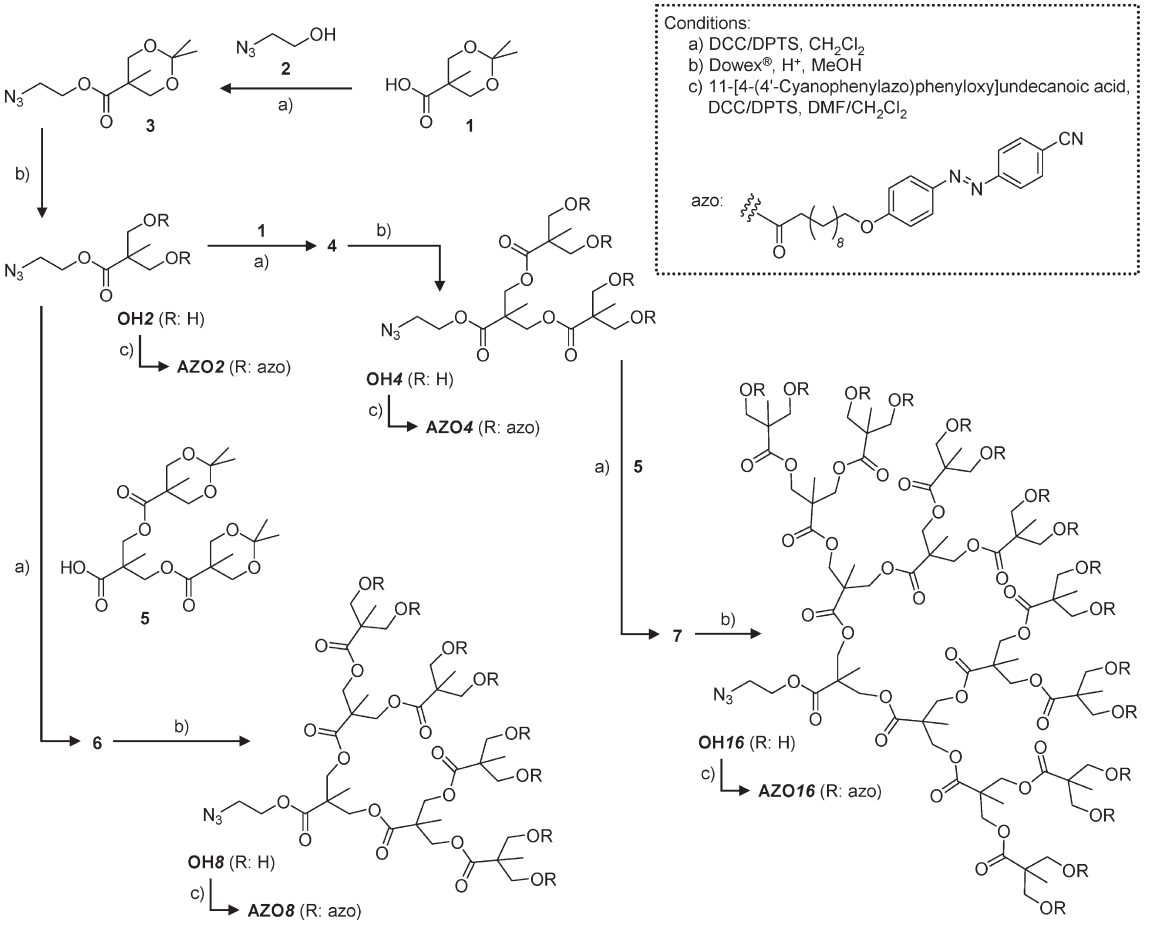


**Scheme 2. Synthesis of PEG-AZO*n* Linear−Dendritic Block Copolymers by Click Chemistry**

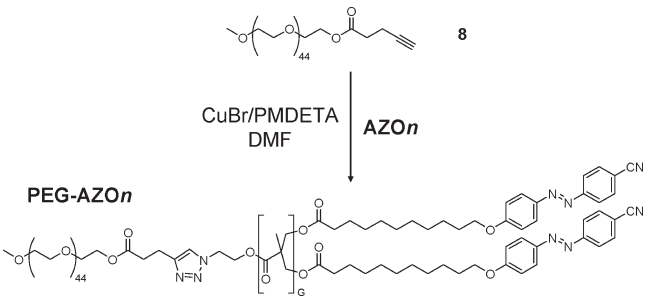


29.45, 29.39, 29.31, 29.15, 29.09, 26.01, 24.84, 17.82, 17.51, 17.41, 17.29. IR (KBr, $cm^{-1}$): 2222, 2106, 1741, 1601, 1255, 846. MALDI-TOF MS (matrix: dithranol) Calcd for $C_{461}H_{557}N_{51}O_{78}$: 8060.95. Found: 8083.0 $[M + Na]^+$. Anal. Calcd for $C_{461}H_{557}N_{51}O_{78}$: C, 68.69; H, 6.96; N, 8.86. Found: C, 68.55; H, 7.02; N, 8.65.

**Synthesis of BCs (PEG-AZO*n*).** ***PEG-AZO2***. A Schlenk flask was charged with the alkyne-functionalized PEG (**8**) (0.205 g, 97.78 $\mu$mol), **AZO*2*** (0.08 g, 81.45 $\mu$mol), and CuBr (23.4 mg, 163.12 $\mu$mol). The flask was closed with a rubber septum and evacuated and backfilled with argon several times. 1,1,4,7,7-Pentamethyldiethylenetriamine (PMDETA) (3.4 $\mu$L, 162.64 $\mu$mol) and deoxygenated DMF (4 mL) were added with an argon-purged syringe, and the flask was further degassed by three freeze−pump−thaw cycles. The reaction mixture was stirred under an argon atmosphere at RT for 18 h. The mixture was diluted with dichloromethane and then passed through a short column of aluminum oxide, using dichloromethane as eluent, to remove copper salts. The solvent was partially evaporated, and the resulting polymer solution was carefully poured into a large volume of cold methanol. **PEG-AZO*2*** was obtained as an orange powder. The final product was dried under vacuum at 40 °C for 48 h. $^1$H NMR (400 MHz, $CDCl_3$, $\delta$): 7.93 (d, $J$ = 8.8 Hz, 8H), 7.78 (d, $J$ = 8.6 Hz, 4H), 7.46 (s, 1H), 7.01 (d, $J$ = 9.0 Hz, 4H), 4.58 (t, $J$ = 5.0 Hz, 2H), 4.50 (t, $J$ = 5.0 Hz, 2H), 4.25−4.13 (m, 6H), 4.04 (t, $J$ = 6.5 Hz, 4H), 3.62 (m, 178H), 3.38 (s, 3H), 3.03 (t, $J$ = 7.2 Hz, 2H), 2.76 (t, $J$ = 7.2 Hz, 2H), 2.24 (t, $J$ = 7.5 Hz, 4H), 1.86−1.77 (m, 4H), 1.62−1.52 (m, 4H), 1.51−1.42 (m, 4H), 1.40−1.20 (m, 23H). IR (KBr, $cm^{-1}$): 2234, 1738, 1602, 1242, 843. Anal. Calcd for $C_{151}H_{255}N_9O_{55}$ C, 58.95; H, 8.35; N, 4.10. Found: C, 59.67; H, 8.20; N, 4.24.

***PEG-AZO4***. Alkyne-functionalized PEG (**8**) (0.10 g, 47.74 $\mu$mol), **AZO*4*** (0.08 g, 40.13 $\mu$mol), CuBr (11.5 mg, 80.17 $\mu$mol), and PMDETA (16.8 $\mu$L, 80.36 $\mu$mol) in DMF (2 mL) were reacted for 30 h according to the cycloaddition procedure described for **PEG-AZO*2***. After purification, **PEG-AZO*4*** was obtained as an orange powder. The final product was dried under vacuum for 48 h. $^1$H NMR (400 MHz, $CDCl_3$, $\delta$): 7.90 (d, $J$ = 8.7 Hz, 16H), 7.78 (d, $J$ = 8.5 Hz, 8H), 7.51 (s, 1H), 7.00 (d, $J$ = 8.9 Hz, 8H), 4.60 (t, $J$ = 5.0 Hz, 2H), 4.51 (t, $J$ = 5.0 Hz, 2H), 4.26−4.12 (m, 14H), 4.03 (t, $J$ = 6.5 Hz, 8H), 3.62 (m, 178H), 3.38 (s, 3H), 3.04 (t, $J$ = 7.2 Hz, 2H), 2.76 (t, $J$ = 7.2 Hz, 2H), 2.29 (t $J$ = 7.5 Hz, 8H), 1.85−1.76 (m, 8H), 1.64−1.52 (m, 8H), 1.50−1.41 (m, 8H), 1.40−1.17 (m, 49H). IR (KBr, $cm^{-1}$): 2234, 1738, 1602, 1246, 857. Anal. Calcd for $C_{209}H_{325}N_{15}O_{65}$ C, 61.41; H, 8.01; N, 5.14. Found: C, 60.48; H, 7.92; N, 5.14.

***PEG-AZO8***. Alkyne-functionalized PEG (**8**) (0.09 g, 42.97 $\mu$mol), **AZO*8*** (0.15 g, 37.35 $\mu$mol), CuBr (10.1 mg, 70.41 $\mu$mol), and PMDETA (14.7 $\mu$L, 70.32 $\mu$mol) in DMF (4 mL) were reacted for 52 h according to the cycloaddition procedure described for **PEG-AZO*2***. After purification, **PEG-AZO*8*** was obtained as an orange powder. The final product was dried

under vacuum for 48 h. $^1$H NMR (400 MHz, $CDCl_3$, $\delta$): 7.90 (d, $J$ = 8.7 Hz, 32H), 7.77 (d, $J$ = 8.5 Hz, 16H), 7.52 (s, 1H), 7.00 (d, $J$ = 9.0 Hz, 16H), 4.61 (t, $J$ = 5.0 Hz, 2H), 4.52 (t, $J$ = 5.0 Hz, 2H), 4.27−4.12 (m, 30H), 4.02 (t, $J$ = 6.5 Hz, 16H), 3.62 (m, 178H), 3.37 (s, 3H), 3.02 (t, $J$ = 7.2 Hz, 2H), 2.76 (t, $J$ = 7.2 Hz, 2H), 2.28 (t, $J$ = 7.5 Hz, 16H), 1.84−1.75 (m, 16H), 1.62−1.52 (m, 16H), 1.50−1.18 (m, 117H). IR (KBr, cm$^{-1}$): 2221, 1742, 1601, 1255, 844. Anal. Calcd for $C_{325}H_{465}N_{27}O_{85}$ C, 63.88; H, 7.67; N, 6.19. Found: C, 63.76; H, 7.78; N, 5.55.

***PEG-AZO16***. Alkyne-functionalized PEG (**8**) (0.07 g, 33.42 $\mu$mol), **AZO*16*** (0.22 g, 27.29 $\mu$mol), CuBr (7.8 mg, 54.37 $\mu$mol), and PMDETA (11.4 $\mu$L, 54.53 $\mu$mol) in DMF (4 mL) were reacted for 72 h according to the cycloaddition procedure described for **PEG-AZO*2***. After purification, **PEG-AZO*16*** was obtained as an orange powder. The final product was dried under vacuum for 48 h. $^1$H NMR (400 MHz, $CDCl_3$, $\delta$): 7.90 (d, $J$ = 8.0 Hz, 64H), 7.75 (d, $J$ = 7.9 Hz, 32H), 7.52 (s, 1H), 7.00 (d, $J$ = 8.1 Hz, 32H), 4.68−4.49 (m, 4H), 4.33−4.08 (m, 62H), 4.05−3.95 (m, 32H), 3.71−3.52 (m, 178H), 3.38 (s, 3H), 3.04−2.95 (m, 2H), 2.79−2.70 (m, 2H), 2.28 (t, $J$ = 6.6 Hz, 32H), 1.84−1.72 (m, 32H), 1.70−1.12 (m, 269H). IR (KBr, cm$^{-1}$): 2227, 1741, 1601, 1256, 850. Anal. Calcd for $C_{557}H_{745}N_{51}O_{125}$ C, 65.88; H, 7.39; N, 7.03. Found: C, 64.72; H, 7.15; N, 6.92.

**Characterization Techniques.** Elemental analyses were performed using a Perkin-Elmer 240C microanalyzer. IR spectra were obtained on a Nicolet Avatar 360-FT-IR spectrophotometer using KBr pellets. $^1$H NMR and $^{13}$C NMR spectra were measured at RT with a Bruker AV-400 spectrometer at 400 MHz for $^1$H and at 100 MHz for $^{13}$C. MALDI-TOF MS was performed on an Autoflex mass spectrometer (Bruker Daltonics). Dithranol was used as a matrix and sodium iodide as a cationic agent matrix. MS data were processed using PolyTools 1.0 (Bruker Daltonics). GPC was carried out on a Waters 2695 liquid chromatography system equipped with a Waters 2420 evaporation light scattering detector using a combination of two Ultrastyragel columns with a pore size of 500 and 10$^4$ Å. Measurements were performed on THF at RT with a flow of 1 mL/min using poly(methyl methacrylate) narrow molecular weight standards. Thermogravimetric analysis (TGA) was performed using a TA Q5000IR instrument at a heating rate of 10 °C min$^{-1}$ under a nitrogen atmosphere. Mesogenic behavior was evaluated by POM using an Olympus BH-2 polarizing microscope fitted with a Linkam THMS600 hot stage. Thermal transitions were determined by DSC using a TA DSC Q-2000 instrument under a nitrogen atmosphere with powdered samples (about 3 mg) sealed in aluminum pans. Glass transition temperatures were determined at the midpoint of the baseline jump, and the mesophase−isotropic phase transition temperature was read at the maximum of the corresponding peaks. XRD measurements were performed with an evacuated Pinhole camera (Anton-Paar) operating with a point-focused Ni-filtered Cu K beam. The patterns were collected on flat photographic films perpendicular to the X-ray beam. Powdered samples of the BCs were placed into quartz Lindemann capillaries (1 mm diameter). Fibers of **PEG-AZO*8*** and **PEG-AZO*16*** were obtained from samples cooled down from the isotropic state to 75 °C and annealed at this temperature for 10 h before drawing. Samples for TEM were prepared in the following way: BCs were dissolved in dichloromethane in order to obtain solutions with a concentration of around 1 mg/mL. Thin films were then prepared on carbon-coated copper grids (previously treated in a UV-ozone chamber for 1 min) by drop-casting at RT. In order to enhance the contrast between the PEG and the azobenzene block, the films were exposed to $RuO_4$ vapor for 1 h.[36] TEM was measured using a JEOL-2000 FXIII electron microscope.

**Optical Measurements in Films.** Thin polymer films for optical measurements were prepared by casting from solutions of the polymer in dichloromethane onto clean glass substrates. Before performing the optical measurements the films were heated up to the isotropic state (10 °C above $T_{S-I}$) for 5 min and quenched to RT. After the thermal treatment, film thickness of about 400 nm was measured using a DEKTAK profilometer. A Varian Cary 500 UV−vis−IR spectrophotometer was used for optical absorption and dichroism measurements. For the latter measurements a linear polarizer was introduced in front of the film. Birefringence ($\Delta n$) measurements were performed using a standard setup reported elsewhere.[21c] The sample was placed between crossed polarizers with their polarization directions at ±45° with the vertical axis and irradiated with vertically polarized 488 nm light from an Ar$^+$ laser. The light from a 633 nm He−Ne laser (1 mW) transmitted through the polarizer−sample−polarizer system was measured with a Si photodetector. It was confirmed that 633 nm light at this power did not introduce any significant change in the optical properties of the film. The transmitted intensity $I$ is given by the equation

$$I = I_0 \sin^2(\pi|\Delta n|d/\lambda) \quad (1)$$

where $I_0$ is the intensity transmitted by the "as-quenched" films between parallel polarizers, $d$ the film thickness, and $\lambda$ the wavelength of the measuring light (633 nm).

## Results and Discussion

**1. Synthesis and Characterization.** A convergent synthetic approach was used for the preparation of a series of linear−dendritic BCs denoted as **PEG-AZO*n*** (Chart 1) employing monomethyl poly(ethylene glycol) ($M_n$ = 2000) as the linear block and the first four generations of bis-MPA based dendrons functionalized at the periphery with 4-cyanoazobenzene units as the dendritic block. Both blocks were linked at the final step of the synthesis by a copper(I)-catalyzed azide−alkyne cycloaddition (Scheme 2). The aliphatic polyester-type dendrons bearing a single azide group at the focal point were synthesized according to a well-known double-stage convergent approach,[35] which is summarized in Scheme 1. Subsequent esterification of the hydroxyl groups at the periphery allowed easy access to functional dendrons that are active for click reactions. In this case, photochromic azobenzene units were grafted onto the periphery of the dendrons through an esterification reaction with an excess of 11-[4-(4′-cyanophenylazo)phenyloxy]undecanoic acid using DCC as the esterification agent and DPTS as the catalyst (Scheme 1).[37] A decamethylenic flexible spacer was chosen to introduce the azo units at the periphery of the dendron in order to increase the solubility of the dendritic building block and to decouple the molecular movements of the bis-MPA based matrix and the photochromic units. Azodendrons, **AZO*n***, were purified by column chromatography and isolated as air-stable orange solids that are soluble in common solvents such as dichloromethane, chloroform, dioxane, and THF.

**AZO*n*** were analyzed by $^1$H NMR, $^{13}$C NMR, and FT-IR as well as by MALDI-TOF MS, GPC, and elemental analysis for full structure characterization. Evidence for the complete functionalization of the periphery of the dendrons was provided by several techniques. The MALDI-TOF mass spectra for **AZO*n*** showed the expected [M]$^+$ ion (in some cases the sodium or potassium adducts were also detected), and peaks corresponding to dendrons with a partial functionalization were not detected (see Supporting Information). The GPC chromatograms of the azodendrons also confirmed the presence of monodisperse compounds. However, as is often the case with dendrimers,[38] clear deviation from the calculated molecular weight was found as a consequence of the different hydrodynamic volume in comparison to more conventional narrow molecular weight standards [in

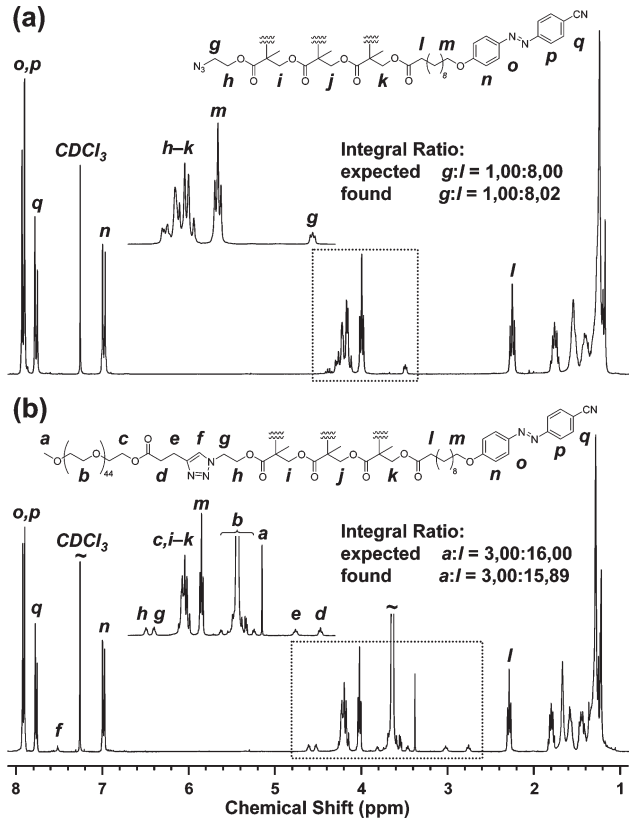


**Figure 1.** $^1$H NMR spectra (400 MHz, $CDCl_3$) of (a) **AZO*8*** azodendron and (b) **PEG-AZO*8*** linear−dendritic BC. The intensity of PEG protons resonance at 3.6 ppm is cut off for clarity.

this case, poly(methyl methacrylate) standards]. The $^1$H NMR spectra of the azodendrons are fully consistent with the proposed chemical structures and confirmed the purity of these compounds. Furthermore, the integral ratios are in good accordance with the expected structure. As an example, the $^1$H NMR spectrum of **AZO*8*** is shown in Figure 1a. The integration ratio between the signals at $\delta$ = 3.45 and 2.35 ppm, which correspond respectively to the methylene unit α to the azide group and the methylene unit α to the carbonyl group of the decamethylenic flexible spacer of the mesogens, also confirmed the complete functionalization of the periphery of the dendron.

The click reaction between the azodendrons and the alkyne-functionalized PEG was performed in DMF at RT using the complex of CuBr with PMDETA as the catalytic system (Scheme 2), which has been shown to give high yields in short reaction times.[39] A slight excess of alkyne-functionalized PEG was used in order to drive click reactions to completion. The excess PEG was easily removed after the reaction by washing with methanol. The reaction time clearly increased with the generation of azodendron involved in the click reaction. This fact can be attributed to the increase in steric hindrance around the azide group as the generation of the azodendritic block increases. In all cases, completion of the reaction was evidenced by the disappearance of the azide signals in the FT-IR spectra of the BCs (see Supporting Information). BCs were also characterized by MALDI-TOF MS. A comparison between the MALDI mass spectra of the alkyne-functionalized PEG and **PEG-AZO*n*** is shown in Figure 2. The spectrum of **PEG-AZO*2***, **PEG-AZO*4***, and **PEG-AZO*8*** each contained a series of peaks 44 Da apart, and these correspond to the sodium adducts of the BCs. In some cases, a series of peaks corresponding to the potassium

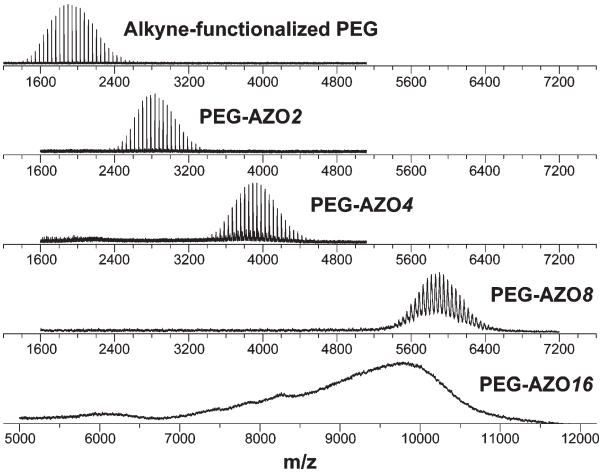


**Figure 2.** MALDI mass spectra (matrix: dithranol) of the alkyne-functionalized PEG and **PEG-AZO*n*** linear−dendritic BCs. Please, note that, for clarity, the scale used in the mass spectrum of **PEG-AZO*16*** is different from the rest of scales.

adducts were also detected. In contrast, the MALDI-TOF spectrum of **PEG-AZO*16*** showed a nonsymmetric peak distribution without individual peak resolution. This BC, which bears the highest generation of the dendritic block, proved to be more difficult to analyze and a higher laser power had to be applied in the MALDI experiments. The unsymmetrical mass spectrum for the BC **PEG-AZO*16*** can be explained by some degradation of the sample due to the high laser power applied for the analysis. The experimental molecular weights obtained from the mass spectra are in good agreement with the calculated molecular weight (Table 1). Moreover, mass spectra confirmed the absence of side products. In particular, signals due to unreacted azodendron were not observed, a situation consistent with the FT-IR spectra. Further evidence for this was provided by the shift in the GPC traces toward higher molecular weight, indicating BC formation and the complete absence of traces of the original blocks. Moreover, an increase in the polydispersity was not observed upon BC formation, a finding that implies that the coupling reaction went to completion (see Supporting Information). The linkage of the blocks to generate the BC was also demonstrated by $^1$H NMR spectroscopy. As an example, the $^1$H NMR spectrum of **PEG-AZO*8*** is shown in Figure 1b. Assignments of the individual peaks were made by comparison with the protons of the PEG block ($H^a$, $H^d$, and $H^e$) and of the azodendron (aromatic protons of the cyanoazobenzene units, $H^m$ and $H^n$). Moreover, the integral ratio of the signals at 3.38 and 2.29 ppm corresponding to the terminal methyl group of the PEG block and the methylene unit linked to the carbonyl group of the decamethylenic flexible spacer is in good agreement with the theoretical value.

**2. Thermal Characterization and Morphological Study.** The thermal stability of the azodendrons and the final BCs was studied by thermogravimetry (Table 2) using powdered samples. All samples studied exhibited a good thermal stability up to ~250 °C, with the onset of decomposition detected at temperatures higher than 300 °C. (Degradation of the azide goup of the azodendrons was detected by FT-IR when heating these materials at temperatures higher than 170 °C. However, a possible weight loss associated with the degradation process of the azide group was not detected in the TGA curves.)

The thermal and mesomorphic properties of the azodendrons and the BCs were studied by DSC, POM, and XRD.

**Table 1. Linear−Dendritic Block Copolymers PEG-AZO*n* Synthesized by Click Chemistry**

| | | MALDI-TOF | | GPC | | | |
|---|---|---|---|---|---|---|---|
| block copolymer | $M_n$(calcd) | $M_n$[a] | PDI[a] | $M_n$[b] | PDI[b] | azodendron block (wt %)[c] | azo content (wt %)[d] |
| **PEG-AZO*2*** | 3077 | 2840 | 1.005 | 5100 | 1.01 | 32 | 14 |
| **PEG-AZO*4*** | 4088 | 3870 | 1.002 | 6400 | 1.02 | 49 | 22 |
| **PEG-AZO*8*** | 6110 | 5930 | 1.001 | 7700 | 1.01 | 66 | 29 |
| **PEG-AZO*16*** | 10 155 | 9118 | 1.016 | 11 000 | 1.02 | 79 | 35 |

[a] Number-average molecular weight ($M_n$) and polydispersity (PDI) of the BCs were calculated from the mass spectra using PolyTools 1.0 (Bruker Daltonics). [b] Relative $M_n$ and PDI to PMMA calibration. [c] Weight percentage of the azodendron block determined by using the calculated-molecular weight of the BC. [d] Weight percentage of the azo chromophoric units (4-oxy-4′-cyanoazobenzene) determined by using the calculated molecular weight of the BC.

**Table 2. Thermal Stability and Transition Temperatures for AZO*n* Azodendrons and PEG-AZO*n* Linear−Dendritic Block Copolymers**

| sample | $T_{onset}$[a] (°C) | thermal transitions[b] (°C) [$\Delta H$ (kJ mol$^{-1}$)] | $\Delta H_{S-I}$/m.u.[c] (kJ mol$^{-1}$) |
|---|---|---|---|
| **AZO*2*** | 302 | I 84 [8.0] SmA 12 [12.1] Cr | 4.0 |
| **AZO*4*** | 321 | I 106 [17.3] SmA 11 g | 4.3 |
| **AZO*8*** | 327 | I 122 [35.3] SmA 17 g | 4.4 |
| **AZO*16*** | 329 | I 139 [67.6] SmA 23 g | 4.2 |
| **PEG-AZO*2*** | 360 | I 13 [44.2] $Cr_1$ 0 [181.1] $Cr_2$ | |
| **PEG-AZO*4*** | 325 | I 47 [12.3] SmA 28 [35.1] $Cr_1$ 24 [157.7] $Cr_2$ | 3.1 |
| **PEG-AZO*8*** | 332 | I 85 [30.3] SmA 6 g | 3.8 |
| **PEG-AZO*16*** | 327 | I 112 [52.7] SmA 17 g | 3.3 |

[a] Decomposition detected in the derivative thermogravimetric curve. [b] Thermal transition determined by DSC form the peak maximum upon cooling (scan rate: 10 °C min$^{-1}$). Calculated molecular weight was used in the calculation of $\Delta H$ (kJ mol$^{-1}$) of the BCs. [c] Enthalpy of the smectic-to-isotropic transition per mesogenic unit.

The phase transitions of both **AZO*n*** and **PEG-AZO*n***, determined upon cooling, are summarized in Table 2. The azodendrons exhibit fan-shaped and homeotropic textures, characteristic of a smectic A mesophase (see Supporting Information). The lamellar nature of the mesophase was confirmed by XRD. The wide-angle X-ray scattering (WAXS) patterns of the azodendrons showed the typical diffuse halo at 4.5 Å, associated with the average lateral distance between mesogens. A sharp halo corresponding to the first-order reflection of the smectic layers was detected at 46 Å (in the case of **AZO*16***, the first- and second-order reflection from the smectic layer spacing were observed but only the second order could be measured). Considering the extended molecular length of the azodendron (about 35 Å by Dreiding stereomodels), the layer spacing is explained by an orthogonal smectic mesophase having a bilayer structure with interdigitation of the mesogenic units.[40] **AZO*2*** presents smectic mesomorphism when cooled below $T_{I-S}$ and crystallizes at 12 °C (determined from DSC measurements, Figure 3a). On cooling, **AZO*4***, **AZO*8***, and **AZO*16*** do not crystallize but solidify to form a supercooled smectic glass. The DSC scans corresponding to the second cooling cycle of these compounds (Figure 3a) show a glass transition at around 10−20 °C and a broad isotropic-to-smectic phase transition that varies from about 110 (**AZO*4***) to 140 °C (**AZO*16***). Only the glass transition and the isotropization transition were observed in the heating scan for these materials. The smectic mesophase range increases as the generation (G) of the dendron increases, and this is related to the larger number of mesogens (*n*) in the molecule. On the other hand, the enthalpy change at the isotropic-to-smectic transition per mesogenic unit (Table 2) is about the same order of magnitude for all azodendrons (about 4.2 kJ mol$^{-1}$); therefore, the strength of the interactions between the mesogenic units is similar regardless of the number of units present in the molecule or the size of the bis-MPA dendron. Similar results have already been described for mesogenic dendrimers based on poly(propyleneimine).[38]

DSC traces of BCs **PEG-AZO*n*** upon cooling are shown in Figure 3b. The DSC trace of the nonmesomorphic **PEG-AZO*2*** recorded upon cooling shows two different

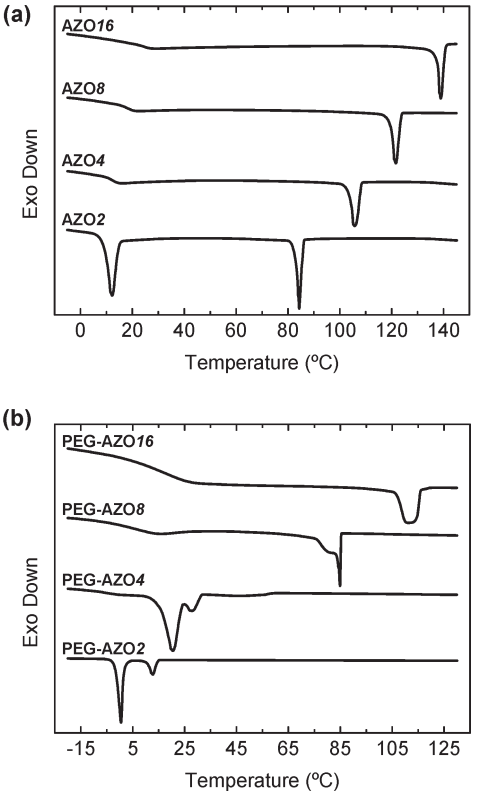


**Figure 3.** DSC traces corresponding to the second cooling scan (10 °C/min) of (a) **AZO*n*** azodendrons and (b) **PEG-AZO*n*** linear−dendritic block copolymers.

crystallization processes: one at 13 °C and the second one at 0 °C. These are tentatively associated with the crystallization of the dendritic block and the PEG block. These two crystallization processes were also observed in the cooling scan of **PEG-AZO*4***. Short range of monotropic mesomorphism was detected by POM prior to crystallization. The isotropic-to-mesophase transition appears as a broad peak at around 50 °C in the DSC trace (Figure 3b). The

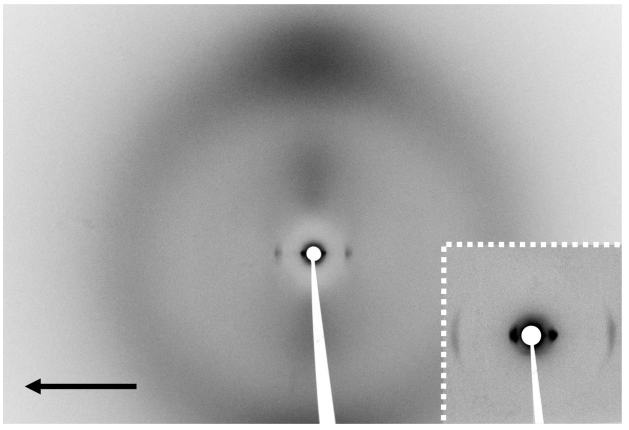

**Figure 4.** X-ray diffraction pattern for fiber sample of **PEG-AZO*16*** linear−dendritic block copolymer at RT. The arrow indicates the fiber drawing direction. Inset: WAXS diffraction pattern of the same sample.

reduction in the crystallization point of the PEG block in **PEG-AZO*2*** and **PEG-AZO*4*** [pure PEG ($M_n$ = 2000) has a crystallization point of 34 °C] may be explained by a confined crystallization of the PEG block[41−43] within the lamellar space between the azo domains. **PEG-AZO*8*** and **PEG-AZO*16*** exhibit enantiotropic mesomorphism and vitrify into a glassy state on cooling (Figure 3b). The mesophase of BCs **PEG-AZO*8*** and **PEG-AZO*16*** has been tentatively assigned as smectic A according to the focal-conic textures observed under the optical microscope (see Supporting Information). On heating, **PEG-AZO*8*** crystallizes (cold crystallization) and melts to give a smectic mesophase at 47 °C; meanwhile, **PEG-AZO*16*** remains amorphous up to the transition to the mesophase, with only a small cold crystallization detected around the glass transition. Both the isotropic-to-smectic transition temperature and the enthalpy per mesogenic unit (Table 2) for the mesomorphic BCs are depressed compared to the liquid crystalline dendrons. These phenomena have been already described for other liquid crystalline coil BCs[24,26a,44−46] and are related to a partial isotropization of the LC structures in the vicinity of the microphase interface.

The crystal structures of **PEG-AZO*2*** and **PEG-AZO*4*** were studied by XRD. The wide-angle region of a powder diffraction pattern obtained from a sample slowly cooled from the isotropic state to RT consists of three strong Bragg reflections at 4.7, 3.8, and 3.2 Å. The first two correspond to (120) and (112 + 032) reflections of monoclinic PEG crystals,[47] and the third one has been tentatively assigned to the crystal structure of the dendritic block. Moreover, the small-angle region of the same diffraction pattern presents a set of peaks with spacings that are in the reciprocal ratio 1:2, indicating a lamellar crystal structure. The layer spacings for **PEG-AZO*2*** and **PEG-AZO*4*** were calculated to be 10.4 and 11.2 nm, respectively. XRD performed on fiber samples of **PEG-AZO*8*** and **PEG-AZO*16*** demonstrated the lamellar microsegregation of these BCs. The diffraction pattern of a fiber sample of **PEG-AZO*16*** is shown in Figure 4. The lateral distance between mesogens in the liquid crystalline domains appears as a pair of diffuse crescents perpendicular to the fiber axis (drawing direction) in the range of 4−5 Å. The small-angle X-ray scattering (SAXS) pattern of the same fiber (inset Figure 4) consists of a pair of arcs parallel to the flow direction corresponding to distances of 86 and 22 Å. The reciprocal ratio between these two maxima is 1:4, indicating a lamellar segregation with a layer distance of 86 Å. The SAXS pattern of a fiber sample of

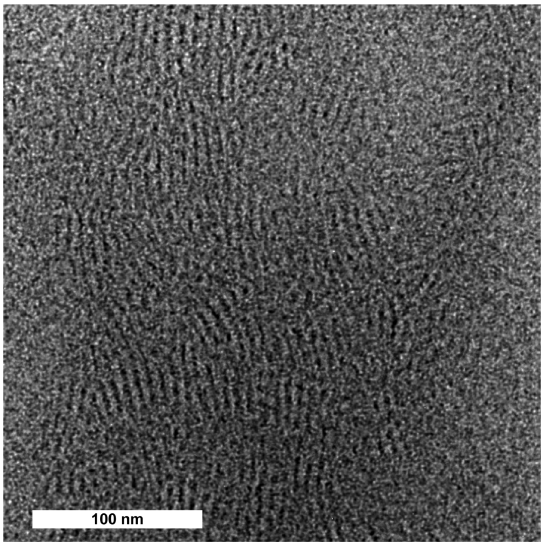


**Figure 5.** TEM image of **PEG-AZO*16*** linear−dendritic BC.

**PEG-AZO*8*** shows scattering signals as arcs perpendicular to the flow direction. The innermost arcs correspond to a distance of 71 Å and are associated with the spacing of the lamellar morphology (SAXS pattern for a fiber sample of **PEG-AZO*8*** and further details about the alignment of **PEG-AZO*8*** and **PEG-AZO*16*** upon fiber drawing are included in the Supporting Information).

In order to support XRD studies of the microphase segregation of **PEG-AZO*n***, TEM was performed on thin films obtained by casting dichloromethane solutions of the BCs onto copper grids. Samples were stained with $RuO_4$ in order to provide contrast for electron imaging. A Typical TEM image of **PEG-AZO*16*** is shown in Figure 5. A lamellar structure with PEG darkened domains was observed in samples without any thermal treatment.[24] Similar morphologies were obtained for the rest of the BCs.

**3. Photoinduced Anisotropy and Dichroism.** In order to study the photo-orientation properties of the azodendrons and BCs, films with homogeneous thickness were prepared by casting dichloromethane solutions of these materials onto clean glass substrates. Prior to any optical study, samples were heated up to the isotropic state (10 °C above $T_{S-I}$) for 5 min and quenched to RT in order to erase any possible effect induced during the film preparation process. Only the films of **PEG-AZO*16*** maintained the initial optical quality after the thermal treatment. Dewetting was observed in the thermally treated films of all the azodendrons and the rest of the BCs, and this prevented us from performing optical studies in these films (dewetting was observed after the thermal treatment even in the films of **AZO*16***). The optical absorption spectrum of a film of **PEG-AZO*16*** after the thermal treatment is shown in Figure 6. The polymer film shows a main absorption band at about 350 nm ($OD_{max}$ = 4 $\mu m^{-1}$) and a tail in the 450 nm region associated with the $\pi-\pi^*$ and $n-\pi^*$ transitions of the *trans* azo moiety, respectively.

Photoinduced anisotropy experiments were carried out in thermally treated films of **PEG-AZO*16*** (400 nm thick) using linearly polarized light of 488 nm (400 mW/cm$^2$). The evolution of photoinduced $|\Delta n|$ in films of **PEG-AZO*16*** as a function of temperature is shown in Figure 7. Experiments were performed at temperatures of 30, 40, 50, 60, and 70 °C (birefringence was not induced at higher temperatures). In every case, films were irradiated for 90 min, kept in darkness at the same temperature for 30 min, and then cooled down

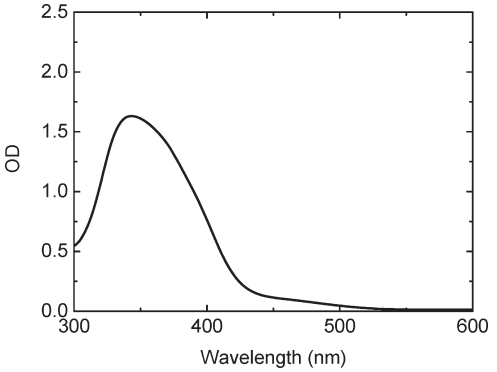


**Figure 6.** Optical absorption of a 400 nm thick film of **PEG-AZO*16*** after thermal annealing at 122 °C for 5 min.

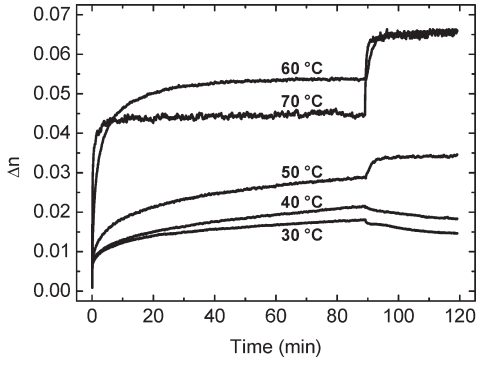


**Figure 7.** Evolution of birefringence of a thin film of **PEG-AZO*16*** measured at different temperatures under 488 nm linearly polarized light after quenching from the isotropic phase to RT. The light is switched off at $t$ = 90 min.

to RT. It can be seen that saturation was not reached (for the exposure time) in experiments at 30−50 °C. On the other hand, $|\Delta n|$ saturates under irradiation at 60 and 70 °C. The saturation value achieved at 60 °C before switching off the 488 nm light was higher than that obtained at 70 °C, although faster evolution toward saturation was achieved at higher temperatures. When the light was switched off, $|\Delta n|$ decreased for samples irradiated at 30 and 40 °C and increased for 50, 60, and 70 °C.

It is well-known that cooperative interactions between chromophores can reinforce the light-induced orientation in liquid-crystalline azopolymers.[4,21c,48] At low temperatures, the molecular mobility is reduced; consequently, the photoinduced reorientation is less efficient, and low values of $|\Delta n|$ are obtained. As the temperature increases, the mobility is enhanced, meaning that higher levels of orientation are reached upon irradiation. However, at higher temperatures, the photoinduced orientation competes with the thermally induced disorder, thus preventing the photoinduction of birefringence above 70 °C. Finally, the increase in birefringence observed after the light is switched off can be attributed to cooperative molecular interactions that enhance the photoinduced molecular order. Higher birefringence values are measured (up to $|\Delta n|$ = 0.093) after the sample was cooled down to RT in the case of the experiments performed at 60 and 70 °C. This feature is related to an increase in the molecular order of the liquid crystalline phase upon cooling. It was confirmed that photoinduced birefringence was stable during several days when the film was stored in darkness.

In order to characterize the photoinduced order, dichroism measurements were performed on this material. The absorption spectra shown in Figure 8 were measured at RT, with light polarized perpendicular and parallel to the 488 nm light polarization direction, in a film irradiated for 90 min at 60 °C, with linearly polarized 488 nm light (400 mW/cm$^2$) kept in darkness at the same temperature for 30 min and then cooled down to RT.

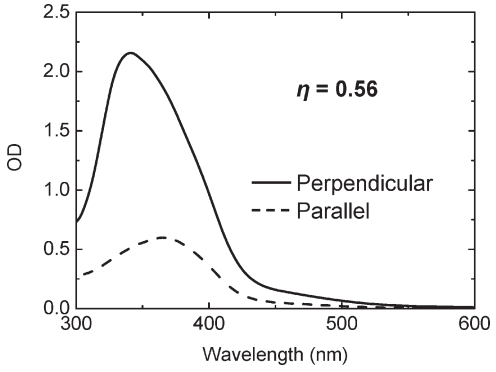


**Figure 8.** Equilibrium polarized absorption spectra measured at RT of **PEG-AZO*16*** and in-plane order parameter after irradiation with 488 nm linearly polarized light at 60 °C for 90 min and subsequent evolution in darkness for 30 min at the same temperature.

The in-plane order parameter $\eta$ can be defined as

$$\eta = (A_\perp - A_\parallel)/(A_\perp + A_\parallel) \quad (2)$$

where $A_\parallel$ and $A_\perp$ are the optical absorptions at $\lambda_{max}$ of the $\pi-\pi^*$ band measured with light linearly polarized in the directions parallel and perpendicular, respectively, to the polarization of the exciting 488 nm light. Stable values of the in-plane order parameter up to 0.56 were obtained in this material.

## Conclusion

A series of well-defined linear−dendritic BCs bearing photoactive units have been synthesized by click chemistry. **PEG-AZO*n*** were obtained by coupling an alkyne-functionalized PEG to the first four generations of aliphatic polyester azodendrons, **AZO*n***, containing a single azide group at their focal point by Huisgen's 1,3-dipolar cycloaddition. The BCs have been fully characterized by NMR, IR, MALDI-TOF, GPC, DSC, and POM. The BC containing two azobenzene units is a crystalline material. However, the BCs bearing 4, 8, and 16 azobenzene units exhibit mesomorphism on optical microscopy. All of the materials self-assemble into a lamellar morphology as evidenced by TEM and XRD studies performed on powder or oriented fiber samples. The photo-orientation properties of **PEG-AZO*16*** under irradiation with 488 nm linearly polarized light have been evaluated. Stable photoinduced order parameters up to 0.56 have been obtained for thin films of **PEG-AZO*16***.

**Acknowledgment.** This work was supported by the MICINN, Spain, under Project MAT2008-06522-C02 and FEDER fundings. C. Sánchez is grateful to MICINN and European Social Foundation for support under the Ramón y Cajal Program. J. del Barrio acknowledges grant from DGA. The authors thank Dr. J. Barberá for helpful discussions on XRD measurements and the Electron Microscope Service of the University of Zaragoza.

**Supporting Information Available:** More details of the synthesis and characterization, IR spectra, GPC chromatograms, MALDI-TOF mass spectra, POM images, and XRD patterns. This material is available free of charge via the Internet at http://pubs.acs.org.

## References and Notes


(1) Hadjichristidis, N.; Pispas, S.; Floudas, G. A. *Block Copolymers: Synthetic Strategies, Physical Properties and Applications*; Wiley-Interscience: New York, 2003.
(2) *Block Copolymers in Nanoscience*; Lazzari, M., Liu, G., Lecommandoux, S., Eds.; Verlag GmbH: Weinheim, Germany, 2006.
(3) Hamley, I. W. *The Physics of Block Copolymers*; Oxford University Press: Oxford, 1998.
(4) Natanshon, A.; Rochon, P. *Chem. Rev.* **2002**, *102*, 4139.
(5) Eich, M.; Wendorff, J. H. *J. Opt. Soc. Am. B* **1990**, *7*, 1428.
(6) Berg, R. H.; Hvilsted, S.; Ramanujam, P. S. *Nature* (*London*) **1996**, *383*, 505.
(7) Yamamoto, T.; Yoneyama, S.; Tsutsumi, O.; Kanazawa, A.; Shiono, T.; Ikeda, T. *J. Appl. Phys.* **2000**, *88*, 2215.
(8) Penner, T. L.; Schildkraut, J. S.; Ringsdorf, H.; Schuster, A. *Macromolecules,* **1991**, *24*, 1041.
(9) Fischer, T.; Läsker, L.; Stumpe, J.; Kostromin, S. G. *J. Photochem. Photobiol. A: Chem.* **1994**, *80*, 453.
(10) Läsker, L.; Fischer, T.; Stumpe, J.; Kostromin, S. G.; Ivanov, S.; Shibaev, V.; Ruhmann, R. *Mol. Cryst. Liq. Cryst.* **1994**, *253*, 1.
(11) Stumpe, J.; Läsker, L.; Fischer, T.; Rutloh, M.; Kostromin, S. G.; Ruhmann, R. *Thin Solid Films* **1996**, *284*, 252.
(12) Eich, M.; Wendorff, J. H.; Reck, B.; Ringsdorf, H. *Makromol. Chem., Rapid Commun.* **1987**, *8*, 59.
(13) Mao, G.; Wang, J.; Clingman, S. R.; Ober, C. K.; Chen, J. T.; Thomas, E. L. *Macromolecules* **1997**, *30*, 2556.
(14) Hayakawa, T.; Horiuchi, S.; Shimizu, H.; Kawazoe, T.; Otshu, M. *J. Polym. Sci., Part A: Polym. Chem.* **2002**, *40*, 2406.
(15) Pavinatto, F. J.; Barletta, J. Y.; Sanfelice, R. C.; Cardoso, M. R.; Balogh, D. T.; Mendonça, C. R.; Oliveira, O. N., Jr. *Polymer* **2009**, *50*, 491.
(16) Jin, M.; Lu, R.; Yang, Q. X.; Bao, C. Y.; Sheng, R.; Xu, T. H.; Zhao, Y. *J. Polym. Sci., Part A: Polym. Chem.* **2007**, *45*, 3460.
(17) Sin, S. L.; Gan, L. H.; Hu, X.; Tam, K. C.; Gan, Y. Y. *Macromolecules* **2005**, *38*, 3943.
(18) (a) Su, W.; Han, K.; Luo, Y.; Wang, Z.; Li, Y.; Zhang, Q. *Macromol. Chem. Phys.* **2007**, *208*, 955. (b) Su, W.; Luo, Y.; Yan, Q.; Wu, S.; Han, K.; Zhang, Q.; Gu, Y.; Li, Y. *Macromol. Rapid Commun.* **2007**, *28*, 1251.
(19) (a) Wang, D.; Ren, H.; Wang, X.; Wang, X. *Macromolecules* **2008**, *41*, 9382–9388. (b) Wang, D.; Lin, J.; Yen, G.; Wang, X. *Polymer* **2009**, *50*, 418.
(20) (a) Breiner, T.; Kreger, K.; Hagen, R.; Häckel, M.; Kador, L.; Müller, A. H. E.; Kramer, E. J.; Schmidt, H. W. *Macromolecules* **2007**, *40*, 2100–2108. (b) Häckel, M.; Kador, L.; Kropp, D.; Schmidt, H. W. *Adv. Mater.* **2007**, *19*, 227–231. (c) Häckel, M.; Kador, L.; Kropp, D.; Frenz, D.; Schmidt, H. W. *Adv. Funct. Mater.* **2005**, *15*, 1722–1727. (d) Frenz, C.; Fuchs, A.; Schmidt, H. W.; Theissen, U.; Haarer, D. *Macromol. Chem. Phys.* **2004**, *205*, 1246–1258.
(21) (a) Forcén, P.; Oriol, L.; Sánchez, C.; Alcalá, R.; Hvilsted, S.; Jankova, K.; Loos, J. *J. Polym. Sci., Part A: Polym. Chem.* **2007**, *45*, 1899. (b) Forcén, P.; Oriol, L.; Sánchez, C.; Rodrķguez, F. J.; Alcalá, R.; Hvilsted, S.; Jankova, K. *Eur. Polym. J.* **2007**, *43*, 3292. (c) Gimeno, S.; Forcén, P.; Oriol, L.; Piñol, M.; Sánchez, C.; Rodrķguez, F. J.; Alcalá, R.; Jankova, K.; Hvilsted, S. *Eur. Polym. J.* **2009**, *45*, 262–271.
(22) Ikeda, T.; Mamiya, J. I.; Yu, Y. *Angew. Chem., Int. Ed.* **2007**, *46*, 506–528.
(23) (a) Yu, H.; Iyoda, T.; Ikeda, T. *J. Am. Chem. Soc.* **2006**, *128*, 11010. (b) Morikawa, Y.; Kondo, T.; Nagano, S.; Seki, T. *Chem. Mater.* **2007**, *19*, 1540–1542.(c) Morikawa, Y.; Nagano, S.; Watanabe, K.; Kamata, K.; Iyoda, T.; Seki, T. *Adv. Mater.* **2006**, *18*, 883.
(24) Tian, Y.; Watanabe, K.; Kong, X.; Abe, J.; Iyoda, T. *Macromolecules* **2002**, *35*, 3739–3747.
(25) Han, Y. K.; Dufour, B.; Wu, W.; Kowalewski, T.; Matyjaszewski, K. *Macromolecules* **2004**, *37*, 9355.
(26) (a) Li, M. H.; Keller, P.; Albouy, P. A. *Macromolecules* **2003**, *36*, 2284–2292. (b) Deng, W.; Albouy, P.-A.; Lacaze, E.; Keller, P.; Wang, X.; Li, M.-H. *Macromolecules* **2008**, *41*, 2459–2466. (c) Yang, J.; Levy, D.; Deng, W.; Keller, P.; Li, M. H. *Chem. Commun.* **2004**, 4345.
(27) Zhao, Y.; Qi, B.; Tong, X.; Zhao, Y. *Macromolecules* **2008**, *41*, 3823–3831.
(28) (a) Gitsov, I.; Wooley, K. L.; Frechet, J. M. J. *Angew. Chem., Int. Ed. Engl.* **1992**, *31*, 1200. (b) Gitsov, I.; Frechet, J. M. J. *Macromolecules* **1993**, *26*, 6536. (c) Gitsov, I.; Frechet, J. M. J. *Macromolecules* **1994**, *27*, 7309. (d) Gao, Y.; Zhang, X.; Yang, M.; Zhang, X.; Wang, W.; Wegner, G.; Burger, C. *Macromolecules* **2007**, *40*, 2606–2612.
(29) Kolb, H. C.; Finn, M. G.; Sharpless, K. B. *Angew. Chem., Int. Ed.* **2001**, *40*, 2004–2021.
(30) Huisgen, R. *Angew. Chem., Int. Ed.* **1963**, *2*, 565–598.
(31) (a) Lutz, J.-F. *Angew. Chem., Int. Ed.* **2007**, *46*, 1018–1025. (b) Binder, W. H.; Sachsenhofer, R. *Macromol. Rapid Commun.* **2008**, *29*, 952. (c) Fournier, D.; Hoogenboom, R.; Schubert, U. S. *Chem. Soc. Rev.* **2007**, *38*, 1369–1380. (d) Goodall, G. W.; Hayes, W. *Chem. Soc. Rev.* **2006**, *35*, 280–312.
(32) (a) Opsteen, J. A.; van Hest, J. M. C. *Chem. Commun.* **2005**, 57–59. (b) Agut, W.; Taton, D.; Lecommandoux, S. *Macromolecules* **2007**, *40*, 5653–5661. (c) Urien, M.; Erothu, H.; Cloutet, E.; Hiorns, R. C.; Vignau, L.; Cramail, H. *Macromolecules* **2008**, *41*, 7033–7040. (d) Altintas, O.; Hizal, G.; Tunca, U. *J. Polym. Sci., Part A: Polym. Chem.* **2006**, *44*, 5699. (e) Altintas, O.; Yankul, B.; Hizal, G.; Tunca, U. *J. Polym. Sci., Part A: Polym. Chem.* **2006**, *44*, 6458. (f) Durmaz, H.; Dag, A.; Altintas, O.; Erdogan, T.; Hizal, G.; Tunca, U. *Macromolecules* **2007**, *40*, 191. (g) Reynhout, J. C.; Cornelissen, J. J. L. M.; Nolte, R. J. M. *J. Am. Chem. Soc.* **2007**, *129*, 2327. (h) Quemener, D.; Davis, T. P.; Barner,-Kowollik, C.; Stenzel, M. H. *Chem. Commun* **2006**, 5051.
(33) (a) Hua, C.; Peng, S. M.; Dong, C. M. *Macromolecules* **2008**, *41*, 6686–6695. (b) Peng, S. M.; Chen, Y.; Hua, C.; Dong, C. M. *Macromolecules* **2009**, *42*, 104–113.
(34) Alcalá, R.; Giménez, R.; Oriol, L.; Pinol, M.; Serrano, J. L.; Villacampa, A.; Viñuales, A. *Chem. Mater.* **2005**, *19*, 235–246.
(35) Ihre, H.; Hult, A.; Frechet, J. M. J.; Gitsov, I. *Macromolecules* **1998**, *31*, 4061–4068.
(36) Trent, J. S.; Scheinbeim, J. I.; Couchman, P. R. *Macromolecules* **1983**, *16*, 589.
(37) Moore, J. S.; Stupp, S. I. *Macromolecules* **1990**, *23*, 65.
(38) Martín-Rapún, R.; Marcos, M.; Omenat, A.; Serrano, J. L.; Luckhurst, G. R.; Mainal, A. *Chem. Mater.* **2004**, *16*, 4969–4979.
(39) Golas, P. L.; Tsarevsky, N. V.; Sumerlin, B. S.; Matyjaszewski, K. *Macromolecules* **2006**, *39*, 6451.
(40) Shibaev, V.; Bobrosky, A.; Boiko, N. *Prog. Polym. Sci.* **2003**, *28*, 729.
(41) Iyer, J.; Fleming, K.; Hammond, P. T. *Macromolecules* **1998**, *31*, 8757.
(42) Gitsov, I.; Wooley, K. L.; Pavlina, T. I.; Frechet, J. M. J. *Macromolecules* **1993**, *26*, 5621.
(43) Zhu, L.; Cheng, S. Z. D.; Calhoun, B. H.; Ge, Q.; Quirk, R. P.; Thomas, E. L.; Hsiao, B. S.; Yeh, F.; Lotz, B. *Polymer* **2001**, *42*, 5829–5839.
(44) (a) Zhang, W. Y.; Hammond, P. T. *Macromolecules* **1998**, *31*, 711. (b) Anthamatten, M.; Wu, J.; Hammond, P. *Macromolecules* **2001**, *34*, 8574.
(45) Adam, J.; Gronski, W. *Macromol. Rapid Commun.* **1989**, *10*, 553.
(46) Komiya, Z.; Schrock, R. R. *Macromolecules* **1993**, *26*, 1387.
(47) Takahashi, Y.; Tadokoro, H. *Macromolecules* **1973**, *6*, 672.
(48) Kidowaki, M.; Fujiwara, T.; Morino, S.; Ichimura, K.; Stumpe, J. *Appl. Phys. Lett.* **2000**, *76*, 1377.